

Signatures of dynamical tunneling in semiclassical quantum dots

A. Ramamoorthy,¹ R. Akis,¹ J. P. Bird,¹ T. Maemoto,² D. K. Ferry,¹ and M. Inoue²

¹*Nanostructures Research Group, Department of Electrical Engineering, Arizona State University, Tempe, Arizona 85287-5706, USA*

²*Department of Electrical Engineering, Osaka Institute of Technology, 5-16-1 Ohmiya, Asahi-ku, Osaka 535-8585, Japan*

(Received 11 February 2003; published 29 August 2003)

We study transport in large, and strongly open, quantum dots, which might typically be viewed as lying well within the semiclassical regime. The low-temperature magnetoresistance of these structures exhibits regular fluctuations, with just a small number of dominant frequency components, indicative of the presence of dynamical tunneling into regular orbits. Support for these ideas is provided by the results of numerical simulations, which reveal wave function scarring by classically inaccessible orbits, which is found to persist even in the presence of a moderately disordered dot potential. Our results suggest that dynamical tunneling may play a more generic role in transport through mesoscopic structures than has thus far been appreciated.

DOI: 10.1103/PhysRevE.68.026221

PACS number(s): 05.45.Mt, 73.63.Kv

I. INTRODUCTION

Semiconductor quantum dots are the solid-state analog of billiard systems and have been widely studied in recent years as an experimental probe of quantum chaos [1]. Electron transport in these structures involves a process in which electrons are injected into the dot and scatter multiply from its confining walls, before finally escaping to the source or drain reservoirs. The electrical properties of the dots are therefore expected to strongly reflect their classical scattering characteristics, and it is this property that makes them interesting for the study of quantum chaos.

In most discussions of quantum chaos, it is typical to focus on the behavior exhibited by systems in the semiclassical limit, where the size of the dot (L) is much larger than the electron wavelength (λ_F) and its leads support a large number of one-dimensional modes ($W \gg \lambda_F$, where W is the lead width) [2]. Recently, however, we have investigated the transport in quantum dots, intermediate between the semiclassical and quantum limits ($L/\lambda_F < 10$, $W/\lambda_F \sim 1-5$) [3–10]. Crucial to understanding the properties of these structures is the *nonuniform* broadening of their discrete level spectrum, which arises when the dot is coupled to its environment [9–11]. If we consider the case where we start from an initially isolated dot, with a discrete density of states, the effect of opening the leads to the reservoirs is to cause a strong broadening of the majority of these states, while leaving a much smaller subset almost unperturbed [9]. Experimentally, this effect may be probed by the application of a magnetic field, which sweeps the surviving states past the Fermi level, giving rise to reproducible oscillations in the low-temperature conductance [1,7,12]. For semiclassical analysis of this effect, it is important to note that the dots typically exhibit a *mixed* classical phase space, featuring well-defined Kolmogorov-Arnold-Moser (KAM) islands that correspond to periodic orbits [8,13]. While much effort has focused on the fractal conductance fluctuations resulting from this phase space [13–18], we have recently shown that the dominant components of these fluctuations arise from the *dynamical tunneling* of electrons into the KAM islands [8]. The idea is that the tunnel-coupled orbits serve as quasi-bound states of the open dot, and quantization of their action

gives rise to discrete levels that agree with the robust states obtained in quantum-mechanical calculations [6,8]. The dynamical tunneling therefore provides a natural interpretation for the nonuniform level broadening that arises in these structures, and the discrete states that survive the introduction of the coupling are found to have wave functions that are strongly *scarred* by periodic orbits [8]. As such, this behavior shows many similarities with the effect of *resonant trapping*, which is well known from studies of nuclear physics and microwave cavities [19–21], and which occurs in systems in which a small number of localized states are coupled to a continuum.

Here, we explore whether signatures of dynamical tunneling can be observed in much larger quantum dots ($L/\lambda_F \sim 60$), which are very strongly coupled to their reservoirs ($W/\lambda_F \sim 15$). While these structures lie well within the semiclassical limit, we find that their transport characteristics, in fact, show many similarities with those reported in our earlier studies. Their magnetoconductance fluctuations, in particular, exhibit specific frequency components, as found previously in structures where dynamical tunneling is significant [8]. Another interesting effect, and one which appears to be unique to these strongly open dots, is an enhancement of the fluctuation amplitude in the magnetic-field regime where Landau quantization becomes resolved. This behavior is discussed in terms of the ability of the magnetic field to promote electron trapping in the dots, once the curvature of the cyclotron orbits becomes comparable to their size.

II. EXPERIMENT

Quantum dots were formed in the high-mobility two-dimensional electron gas of the InAs/AlSb heterojunction system, by photolithography and wet etching (Fig. 1) [22,23]. In contrast to more widely studied GaAs-based structures [1], the advantage of this material system is its high electron density ($\sim 10^{12} \text{ cm}^{-2}$ at 4.2 K), and correspondingly small Fermi wavelength (25 nm). The mobility of the electron layer ranges from 250 000 to 300 000 $\text{cm}^2/\text{V s}$ at 4.2 K, corresponding to a mean free path of $\sim 4-5 \mu\text{m}$. Three different dots were investigated and their dimensions are listed in Table I (also see Fig. 1), where we also indicate

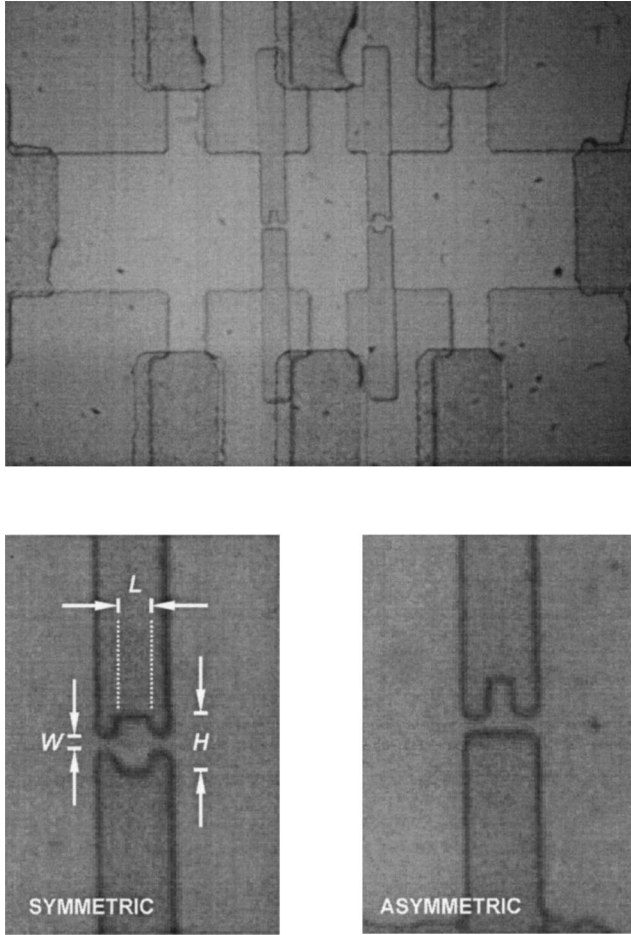


FIG. 1. Micrograph showing the different types of quantum-dot structures studied here.

the notation that we use hereafter to refer to these structures. The samples were mounted on ceramic-bodied chip carriers, and their magnetoresistance was measured in the temperature range from 0.01 to 4.2 K, using standard low-frequency lock-in detection and a constant current of 3 nA.

In Fig. 2, we show the magnetoresistance of dot *A* at a series of different temperatures. Reproducible fluctuations emerge as the temperature is lowered below 1 K, and, at low magnetic fields, these are superimposed on a monotonically

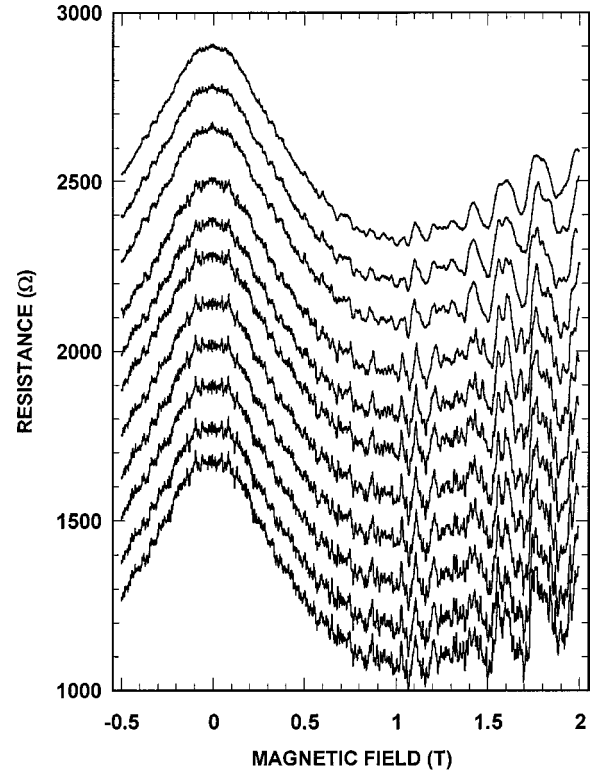


FIG. 2. Magnetoresistance for a single dot at different temperatures. From top to bottom, temperatures are 4.2, 2.4, 1.8, 1.1, 0.92, 0.7, 0.5, 0.4, 0.3, 0.2, and 0.12 K. The various plots have been offset for clarity.

varying background. At higher fields, the fluctuations coexist with the Shubnikov–de Haas oscillations associated with the depopulation of successive Landau levels. Note the low resistance of this dot, which indicates that its leads support a large number of modes. This was found to be the case for all three dots investigated here, as we indicate in Table I, where we have estimated the *minimum* mode number from the resistance of the different dots. In Fig. 3, we show, in an expanded view, the low-field fluctuations in the three dots. The symmetry of these data around zero magnetic field is expected [24] from the Landauer–Büttiker formula, and demonstrates the reproducibility of our measurements. The large amplitude of fluctuation exhibited by each of these curves

TABLE I. Parameters for the different dots studied in the experiment.

Dot	Design	L (μm)	H (μm)	W (μm)	L/λ_F	W/λ_F	$R_{4.2\text{K}}^a$ (Ω)	N^b	δg_{rms}^c (e^2/h)
<i>A</i>	Symmetric	1.5	3.1	0.9	60	36	1658	16	0.12
<i>B</i>	Symmetric	1.6	3.0	1.2	64	48	970	26	0.37
<i>C</i>	Symmetric	2.0	3.0	1.2	80	48	879	30	0.28

^aThe zero-field resistance of the dot, measured at 4.2 K.

^bThe mode number in the point contact leads. This is estimated by assuming that the measured dot resistance is dominated by the contribution from the point contacts, which are taken to add Ohmically for the determination of the mode number.

^cRoot-mean-square amplitude of fluctuation at 0.01 K. The field range from -0.5 to $+0.5$ T was used for this calculation.

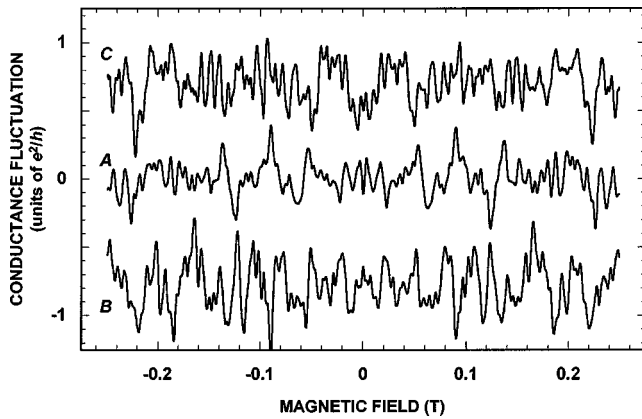


FIG. 3. Conductance fluctuations in the three different dots. The fluctuations were obtained by subtracting a slowly varying background, similar to that apparent in Fig. 2, from the original magnetoresistance. Curves for dots *B* and *C* are offset for clarity.

(Table I) is suggestive of a high degree of electron phase coherence at this temperature [25,26].

It is clear from the data presented in Fig. 3 that, even in the large and strongly coupled dots that we study, the conductance fluctuations exhibit a quasiregular nature. Such behavior is well known from previous investigations of smaller dots [3,4], and has recently been attributed to the dynamical tunneling of electrons into orbits lying on KAM islands [8]. The observation of such quasiperiodic behavior here suggests that the dynamical tunneling is not limited to small dots, but can also occur in structures considered to lie in the semiclassical limit. This is one of the issues that we explore in our numerical simulations of these structures below.

The large dots that we study also provide a useful opportunity to investigate the details of electron interference in the regime where the Landau quantization is well resolved. This regime is indicated in experiment by the emergence of Shubnikov–de Haas oscillations in the magnetoresistance, which are well known to be periodic in the inverse magnetic field. The oscillations are most clearly observed in the higher-temperature traces of Fig. 2, but are obscured by fluctuations at lower temperatures. The amplitude of these fluctuations actually increases with magnetic field in this regime, which behavior can be seen more clearly in Fig. 4. Note, in particular, the data for dot *C* in this figure, which show fluctuations whose amplitude exceeds $50e^2/h$ at the highest magnetic fields [27]. This behavior is quite distinct from that found in previous studies [28,29], which have explored the evolution of the fluctuations with magnetic field in dots coupled to their reservoirs by few-mode leads.

III. ANALYSIS

To explore the origins of the behavior revealed in our experiments, we have performed numerical simulations of magnetotransport in the dot geometry shown as an inset to Fig. 5. The dot is defined by hard walls, which we believe should reasonably approximate the potential in the etched dots that we study here. The corners of this dot are rounded for consistency with the scanning electron microscopy im-

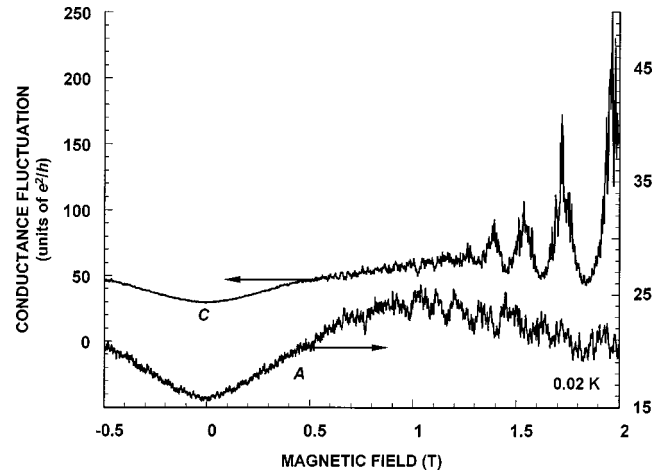


FIG. 4. Low-temperature magnetoresistance of dots *A* and *C*, showing the enhancement of the fluctuations at high magnetic fields.

ages in Fig. 1, and we have also included a random background potential, of maximum amplitude 2 meV, at the bottom of the dot. This last feature is considered to be necessary for calculations of such large dots. The transmission properties of the dot are calculated numerically using a transfer-matrix method, which we have previously applied successfully to our studies of smaller structures [3–10]. Due to difficulties associated with implementing this method in very large dots, the dot dimensions in Fig. 6 are roughly two-thirds of those studied in our experiment. The Fermi energy is also somewhat smaller (84 meV, as opposed to an experimental value of 95 meV), so we emphasize that we do not expect our calculations to provide exact, quantitative, agreement with the results of experiments. Nonetheless, we believe that the structure shown in Fig. 5 does provide the basis for a meaningful system for a qualitative comparison with the results of experiment.

In Fig. 5, we show the calculated magnetoresistance of

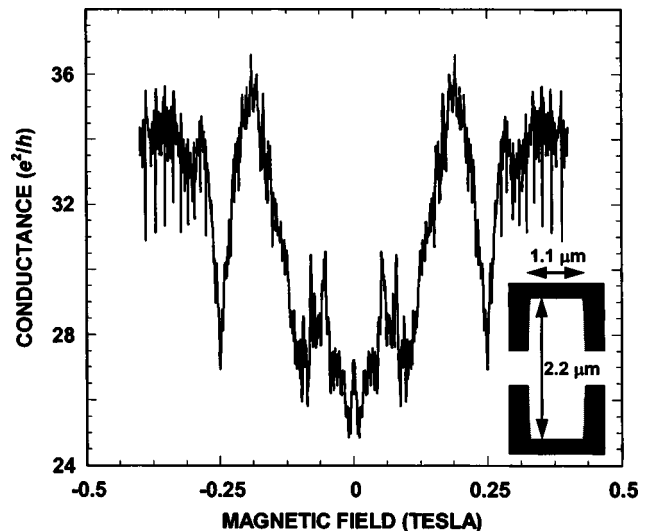


FIG. 5. Calculated magnetoconductance of the dot shown as an inset.

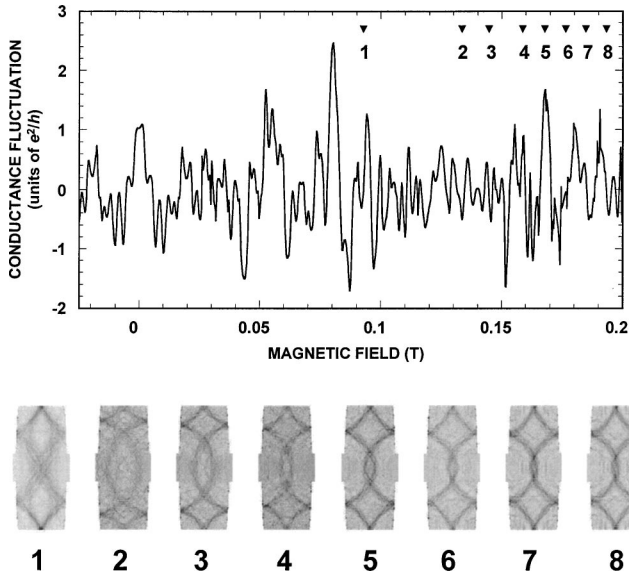


FIG. 6. The upper panel shows calculated conductance fluctuations from Fig. 5 over a smaller range of magnetic field. The numbered symbols plotted on the graph indicate the magnetic fields at which the wave function of the open dot takes the form indicated in the panels at the bottom of the figure.

the dot, whose leads support 19 propagating modes for the Fermi energy that we consider. As with our experimental traces, we see that quasiperiodic fluctuations are superimposed upon larger scale background features in the magnetoconductance. In the upper panel of Fig. 6, we focus on the low-field range of these data, having subtracted out the background variation. The resulting curve is quite reminiscent of the experimental data plotted in Fig. 3. The fluctuation amplitude is somewhat larger, but this can be partly attributed to the fact that we have not included any inelastic scattering or thermal broadening in our calculations.

In previous studies of much smaller dots, we have found that the periodicities evident in their magnetoconductance fluctuations are strongly correlated with the appearance of groups of conductance resonances, spaced quite regularly in magnetic field [3–5]. These resonances in essence form a framework over which the fluctuations are draped. We have also found that resonant states belonging to a particular group all appear to have their amplitude maximized along the same classical periodic orbit. The results of Fig. 6 show that such resonance effects can still be observed at the much larger energy and size scales that we consider here. Note, in particular, the points labeled 1 through 8 in the upper panel of Fig. 6. The open-dot wave functions corresponding to these magnetic-field values are also shown in Fig. 6. In each of the wave functions (which were calculated using the method discussed in Ref. [3]), the quantum mechanical amplitude is concentrated along a classical periodic orbit that forms a double-diamond-like pattern. The orbits themselves are not connected directly to the leads but are instead classically inaccessible to electrons injected into the dot. This feature suggests that the scars are generated by the dynamical tunneling of electrons into these orbits, as we discussed previously for much smaller dots [8]. In Ref. [8], it was argued

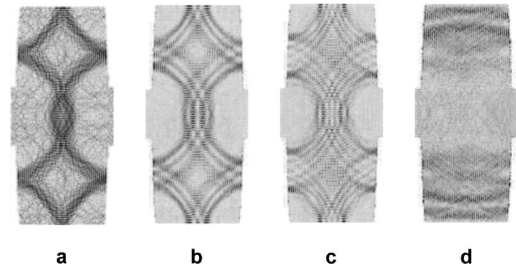


FIG. 7. Calculated eigenfunctions of the *closed* quantum dot, formed by closing off the dot leads, at several different magnetic fields. See text for further details.

that the energy scale on which the scars recur is determined by a quantization of the action of the associated semiclassical orbits. In Fig. 6, it can be seen that the orbits that give rise to the scarring are not exactly identical, due to the increased cyclotron curvature at higher magnetic fields. Consequently, the field scale for recurrence of the scars evolves with the magnetic field itself, decreasing from 40 mT for the first recurrence to a roughly constant period of 9 mT for the last five scars.

As we illustrate in Fig. 7, there is a direct correspondence between the scarred wave functions of the open dot and the eigenstates of the corresponding closed structure. In Fig. 7(a), we show one such eigenstate, computed at a magnetic field of 175 mT. This state corresponds almost exactly with the wave function labeled 6 in Fig. 6. (It should be pointed out that, unlike the open-dot calculations, this eigenstate was computed without any background disorder. Thus, even with relatively small disorder, we see that pure eigenstates can still be selectively excited in transport through the open dot.) In Figs. 7(b) and 7(c), we show the calculated eigenfunctions at magnetic fields of 182 and 190 mT, respectively. While closely related to the scarred eigenstate in Fig. 7(a), these eigenfunctions have additional transverse modes, running across the periodic orbit that gives rise to their scarring. In Figs. 7(b) and 7(c), the transverse mode number (m) is equal to 2 and 4, respectively, and, although not shown here, we have also observed scars for which $m=1, 3$, and 5. As with the basic scar of Fig. 7(a), we find that these higher-order features also recur with magnetic field, although the associated conductance resonances are less pronounced. The magnetic-field periodicity of the recurrence increases slightly with m , with $\Delta B \sim 10$ mT for $m=4$. The existence of such families of scars is actually expected from semiclassical periodic-orbit theory [30], and we have previously found evidence [6,8] for a similar shell structure in a dot with an area 25 times smaller than that considered here. In this structure, however, only states with $m=0$ and 1 were observed. As m increases, it can be seen from Fig. 7 that the associated scars develop a larger lateral spread, and, in such cases, there is a greater overlap of the wave function with regions beyond the KAM island. This in turn permits faster tunneling, thereby weakening the associated transmission resonances. The point to note here is that, in the large dots that we consider, higher values of m can actually be achieved before this leakage becomes too large.

In our discussion thus far, we have focused on the scars

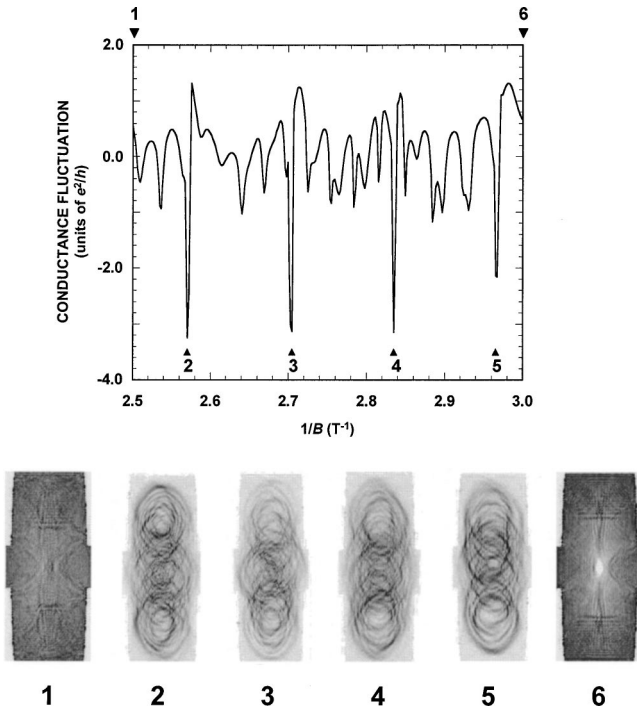


FIG. 8. The upper panel plots the high-field fluctuations from Fig. 5 as a function of *inverse* magnetic field. The numbered symbols plotted on the graph indicate the magnetic fields at which the wave function of the open dot takes the form indicated in the panels at the bottom of the figure.

observed at magnetic fields in excess of 100 mT. The double-diamond-like scars of Figs. 7 and 8 are not observed at fields much lower than this, since the Lorentz force is required to establish these orbits. Evidence for scarring is observed at low magnetic fields, and in this regime tends to be associated predominantly with bouncing-ball orbits. An example of this behavior is shown in Fig. 7(d), which shows the result of a calculation of the closed-dot wave function at a magnetic field of 31 mT.

In the opposite limit of increasing magnetic field, interesting behavior is observed as the Landau-level quantization begins to become resolved. As an illustration of this, in the upper panel of Fig. 8 we replot the high-field data from Fig. 5, this time showing the variation of the conductance fluctuations with *inverse* magnetic field. A set of periodically spaced minima are observed in the data, which we label as points 2 through 5. Away from the minima (and any other resonances), we find that the wave function of the open dot generally exhibits a form quite similar to that shown in the panels labeled 1 and 6 in Fig. 8. Note in these two panels how the transport is mediated by skipping orbits, which couple directly from the leads into the dot. At the minima labeled 2 through 5, however, the corresponding wave functions are dominated by groups of circular orbits that fill the center of the dot, and which are *completely disconnected* from the leads. This periodic switching in inverse magnetic field, from extended edge states to localized bulk orbits, is the quantum-dot analog of the Shubnikov–de Haas effect, more typically observed in two-dimensional electron systems [24]. In the quantum-dot version of this effect, the suggestion

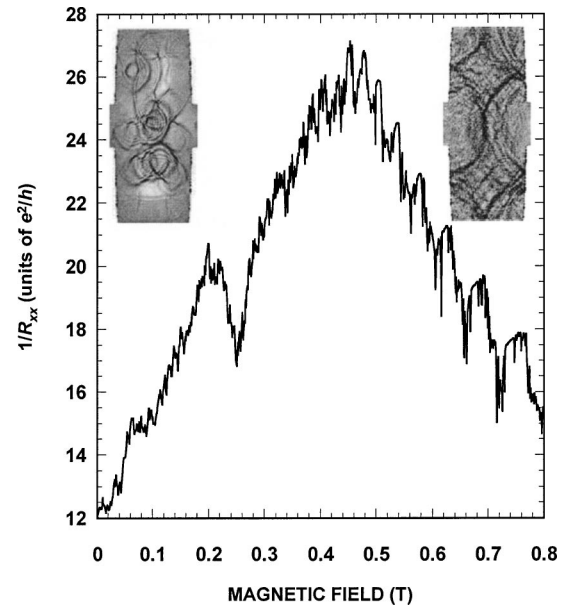


FIG. 9. Calculated magnetoconductance of a dot with a similar geometry to that considered in Fig. 5, but with a background disorder potential of maximum amplitude 20 meV. The left inset shows the wave function of the open dot at a magnetic field of 0.66 T, while the right inset shows the wave function at a magnetic field of 0.18 T, for the purpose of comparison with the results of Fig. 6.

of panels 2 through 5 of Fig. 8 is that Landau-level depopulation is accompanied by the dynamical tunneling of electrons into localized orbits at the center of the dot.

One of the striking features of our experiment, was found to be a large enhancement of the fluctuation amplitude, which occurs in the regime where the Landau quantization becomes resolved (Fig. 4). While some evidence for this behavior can be seen already in our simulations (see Fig. 8), it is shown more clearly in Fig. 9. Here, we have calculated the variation of the longitudinal resistance [23,27]

$$R_{xx} = \frac{h}{e^2} \frac{N-T}{NT}, \quad (1)$$

where T is the transmission coefficient of the dot and N is the number of modes (essentially the number of Landau levels) that are available to couple to the dot from the reservoirs. The conductance ($1/R_{xx}$) derived from this component should be compared with that which we plot in Fig. 4. Similar to the behavior found in experiment, our calculations show that the amplitude of the conductance fluctuations is relatively small at low magnetic fields, but that it increases as the Shubnikov–de Haas oscillations onset. To obtain the data shown in Fig. 9, we have had to increase the magnitude of the disorder potential to about 20 meV, an order of magnitude larger than that considered in Fig. 5. Our earlier conclusions seem to remain valid in this case, however, and in the insets to Fig. 9 we show examples of scarring behavior similar to that found earlier.

IV. DISCUSSION AND CONCLUSIONS

The main objective of this work is to address the extent to which the transport description that we have developed in

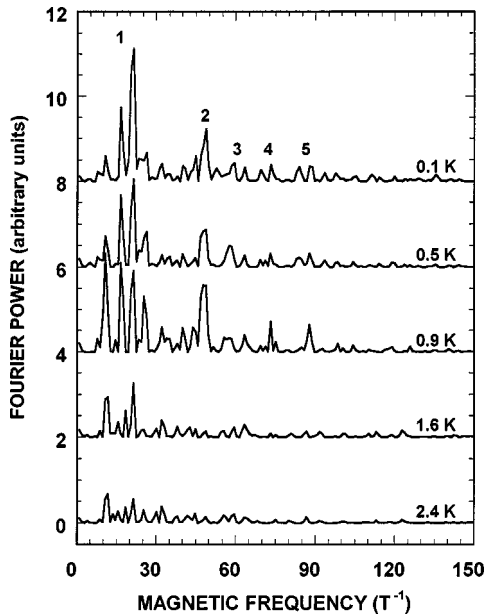


FIG. 10. Fourier power spectra of the conductance fluctuations in dot A at several different temperatures (indicated). Successive curves are offset for clarity.

studies of smaller dots [3–10] is relevant to the discussion of much larger, strongly open, structures. An important conclusion that followed from our earlier work, is that transport through open dots can be dominated by the dynamical tunneling of electrons into classically inaccessible, regular orbits [8]. Quantization of these semiclassical orbits gives rise to a series of discrete energy levels (and associated scarring of the wave function), which are only weakly broadened by the presence of the coupling between the dot and its reservoirs. The key experimental result associated with the dynamical tunneling is the observation of quasiperiodic fluctuations, dominated by just a small number of frequency components, in the conductance of the dot [8]. Perhaps somewhat surprisingly, similarly regular fluctuations were also observed in the large dots that we study here (Fig. 3), suggesting that dynamical tunneling may even be important for transport in these structures. Indeed, as we illustrate in Fig. 10, a Fourier analysis of the conductance fluctuations in these dots typically reveals the presence of a small number of frequency components, reminiscent of the behavior found in Refs. [3–6].

Numerical evidence for the role of dynamical tunneling in these large dots is provided in Figs. 6–8, which show the results of numerical calculations of a similar device to that studied in experiment. The characteristic signature of dynamical tunneling is the presence of wave function scars, whose classical orbits are *inaccessible* to electrons injected into the dot from the leads. The various scars shown in Figs. 6 and 7 clearly show this property. Previously [5,31], we have shown that such isolated scars arise from the diffraction of electron waves, as they are injected into the dot from the leads. This diffraction is understood to be a consequence of the fact that, in the case where the leads support a small number of modes, the lead width is comparable to the electron wavelength. While in the case of interest here the leads

in fact support many modes (more than 10), the suggestion of Figs. 6 and 7 is that the diffraction effects remain significant.

An interesting feature of our experiment was found to be an enhancement of the conductance fluctuation amplitude at high magnetic fields where the Landau quantization becomes resolved (Fig. 4). This effect is reproduced in our numerical simulations (Fig. 9), which also show that the scarring effects tend to become more clearly resolved as the magnetic field is increased (Fig. 6). We believe that the increased amplitude of the conductance fluctuations at higher field may therefore be due to the ability of the magnetic field to promote more effective electron trapping in these very open dots.

A couple of further points are worth emphasizing here. The first is that the key feature required for dynamical tunneling is the presence of periodic orbits at the center of some KAM island. It has been pointed out in the literature that the soft confining walls generic to split-gate quantum dots often give rise to such KAM features, typically giving rise to a *mixed* phase space. As the results presented here suggest, however, the presence of soft walls is *not* a prerequisite for the tunneling behavior. The experimental work presented here is performed on dots that are formed by etching of the semiconductor substrate and can therefore be expected to have relatively hard walls [32]. Similarly, our numerical simulations *assume* a hard-walled system, but in spite of this they show clear evidence for scarring due to classically inaccessible orbits. The point is that, even for a hard-walled structure such as that considered in our calculations, the perturbing presence of the leads [9] tends to set up a mixed phase space, which is therefore a quite generic property of open systems. Another important point to note is that, while we have considered differing degrees of disorder in our calculations, we have found the effects that we discuss to be quite robust to the presence of this disorder.

While our discussion has focused on the influence of dynamical tunneling in open quantum dots, many of our conclusions are consistent with those obtained in generic studies of open scattering billiards [33–35]. Bäcker *et al.* [33], for example, have studied the eigenstates of the cosine billiard, and have shown that these are broadened in a nonuniform manner when the billiard is connected to semi-infinite leads. The magnitude of the resultant broadening can be quantified in terms of a parameter η [33] that expresses the degree of overlap of the cavity eigenfunctions with the leads. Consistent with the conclusions of Ref. [9], the authors showed that the weakest broadening arises for those states whose wave functions exhibit the signatures of periodic orbits, which are classically inaccessible to particles injected into the billiard from the leads. In other related work, the classical analog of the scattering matrix has been formulated and has been applied to the discussion of transport in quantum systems whose classical counterparts exhibit purely chaotic [34] or mixed [34,35] dynamics. In chaotic systems, good correspondence between the predictions of the classical and quantum calculations was reported when the billiard was coupled to leads that support a large number of modes. In mixed systems, however, additional structure, absent in the classical

formulation of the scattering matrix, was found to be present in the quantum counterpart due to dynamical tunneling [35]. Of particular importance for our study here, the tunneling-related features were even found to be present when the cavity leads were configured to support as many as 20 modes, similar to the situation in our experiments (see Table I).

In conclusion, we have studied the transport in large, and strongly open, quantum dots, which might typically be viewed as lying well within the semiclassical regime. We found that the low-temperature magnetoresistance of these structures exhibits regular fluctuations, with just a small number of dominant frequency components, indicative of the presence of dynamical tunneling into regular orbits. Support

for these ideas appears to be provided by the results of numerical simulations, which reveal wave function scarring by classically inaccessible orbits, which is even found to persist in the presence of a moderately disordered dot potential. Our results suggest that dynamical tunneling may play a more generic role in transport through mesoscopic structures than has thus far been appreciated.

ACKNOWLEDGMENTS

Work at ASU is sponsored by the Office of Naval Research and the Department of Energy NSET program Grant No. (DE-FG03-01ER45920, J.P.B.).

-
- [1] For a recent review, see J. P. Bird, *J. Phys.: Condens. Matter* **11**, R413 (1999).
- [2] See, for example, R. A. Jalabert, H. U. Baranger, and A. D. Stone, *Phys. Rev. Lett.* **65**, 2442 (1990).
- [3] R. Akis, D. K. Ferry, and J. P. Bird, *Phys. Rev. B* **54**, 17 705 (1996).
- [4] J. P. Bird, R. Akis, D. K. Ferry, Y. Aoyagi, and T. Sugano, *J. Phys.: Condens. Matter* **9**, 5935 (1997).
- [5] R. Akis, D. K. Ferry, and J. P. Bird, *Phys. Rev. Lett.* **79**, 123 (1997).
- [6] J. P. Bird, R. Akis, D. K. Ferry, D. Vasileska, J. Cooper, Y. Aoyagi, and T. Sugano, *Phys. Rev. Lett.* **82**, 4691 (1999).
- [7] J. P. Bird, R. Akis, and D. K. Ferry, *Phys. Rev. B* **60**, 13 676 (1999).
- [8] A. P. S. de Moura, Y.-C. Lai, R. Akis, J. P. Bird, and D. K. Ferry, *Phys. Rev. Lett.* **88**, 236804 (2002).
- [9] R. Akis, J. P. Bird, and D. K. Ferry, *Appl. Phys. Lett.* **81**, 129 (2002).
- [10] J. P. Bird, R. Akis, D. K. Ferry, A. P. S. de Moura, Y.-C. Lai, and K. M. Indlekofer, *Rep. Prog. Phys.* **66**, 583 (2003).
- [11] I. V. Zozoulenko and K.-F. Berggren, *Phys. Rev. B* **56**, 6931 (1997).
- [12] I. V. Zozoulenko, A. S. Sachrajda, C. Gould, K.-F. Berggren, P. Zawadzki, Y. Feng, and Z. Wasilewski, *Phys. Rev. Lett.* **83**, 1838 (1999).
- [13] R. Ketzmerick, *Phys. Rev. B* **54**, 10 841 (1996).
- [14] A. P. Micolich, R. P. Taylor, R. Newbury, J. P. Bird, R. Wirtz, C. P. Dettmann, Y. Aoyagi, and T. Sugano, *J. Phys.: Condens. Matter* **10**, 1339 (1998).
- [15] A. S. Sachrajda, R. Ketzmerick, C. Gould, Y. Feng, P. J. Kelly, A. Delage, and Z. Wasilewski, *Phys. Rev. Lett.* **80**, 1948 (1998).
- [16] Y. Takagaki and K. H. Ploog, *Phys. Rev. B* **61**, 4457 (2000).
- [17] Y. Takagaki, M. Elhassan, A. Shailos, C. Prasad, J. P. Bird, D. K. Ferry, K. H. Ploog, L.-H. Lin, N. Aoki, and Y. Ochiai, *Phys. Rev. B* **62**, 10 255 (2000).
- [18] A. P. Micolich, R. P. Taylor, A. G. Davies, J. P. Bird, A. Ehlert, T. M. Fromhold, R. Newbury, H. Linke, L. D. Macks, W. R. Tribe, E. H. Linfield, and D. A. Ritchie, *Phys. Rev. Lett.* **87**, 036802 (2001).
- [19] For a review of resonance trapping, see I. Rotter, *Rep. Prog. Phys.* **54**, 635 (1991).
- [20] Y.-H. Kim, M. Barth, H.-J. Stöckmann, and J. P. Bird, *Phys. Rev. B* **65**, 165317 (2002).
- [21] R. G. Nazmitdinov, K. N. Pichugin, I. Rotter, and P. Šeba, *Phys. Rev. B* **66**, 085322 (2002).
- [22] T. Maemoto, H. Dobashi, S. Izumiya, K. Yoh, and M. Inoue, *Jpn. J. Appl. Phys., Part 1* **33**, 7204 (1994).
- [23] T. Maemoto, T. Kobayashi, T. Karasaki, K. Kita, S. Sasa, M. Inoue, K. Ishibashi, and Y. Aoyagi, *Physica B* **314**, 481 (2002).
- [24] D. K. Ferry and S. M. Goodnick, *Transport in Nanostructures* (Cambridge University Press, Cambridge, 1997).
- [25] J. P. Bird, K. Ishibashi, D. K. Ferry, Y. Ochiai, Y. Aoyagi, and T. Sugano, *Phys. Rev. B* **51**, R18 037 (1995).
- [26] D. P. Pivin, Jr., A. Andresen, J. P. Bird, and D. K. Ferry, *Phys. Rev. Lett.* **82**, 4687 (1999).
- [27] Some caution should be exercised here. At low magnetic fields, the four-terminal measurement that we use is effectively equivalent to a two-terminal one, and the resistance is directly related to the transmission coefficient of the dot. At higher fields, however, where edge states begin to become resolved, the measured resistance $R_{xx} = (h/e^2)[(N-T)/NT]$ (see Ref. [23]). Here, N is the number of occupied Landau levels and T is the number of these that are transmitted by the dot, so that R_{xx} is not simply related to T in this regime.
- [28] C. M. Marcus, A. J. Rimberg, R. M. Westervelt, P. F. Hopkins, and A. C. Gossard, *Surf. Sci.* **305**, 480 (1994).
- [29] J. P. Bird, K. Ishibashi, D. K. Ferry, Y. Aoyagi, T. Sugano, and Y. Ochiai, *Phys. Rev. B* **52**, 8295 (1995).
- [30] M. C. Gutzwiller, *Chaos in Classical and Quantum Mechanics* (Springer, New York, 1990).
- [31] R. Akis, J. P. Bird, and D. K. Ferry, *J. Phys.: Condens. Matter* **8**, L667 (1996).
- [32] Regular conductance fluctuations have also been reported in experimental studies of etched, InGaAs quantum dots: K. M. Connolly, D. P. Pivin, Jr., D. K. Ferry, and H. H. Wieder, *Superlattices Microstruct.* **20**, 307 (1996).
- [33] A. Bäcker, A. Manze, B. Huckstein, and R. Ketzmerick, *Phys. Rev. E* **66**, 016211 (2002).
- [34] G. A. Luna-Acosta, J. A. Méndez-Bermúdez, P. Šeba, and K. N. Pichugin, *Phys. Rev. E* **65**, 046605 (2002).
- [35] J. A. Méndez-Bermúdez, G. A. Luna-Acosta, P. Šeba, and K. N. Pichugin, *Phys. Rev. E* **66**, 046207 (2002).